Automated Simulation and Analysis of Electrostatic Micromotors

T. B. Johansson, K. Hameyer, R. Belmans
Katholieke Universiteit Leuven, E.E. Dept., Div. ESAT/ELEN

Industry's interest in micro electro-mechanical systems is rapidly growing. The very small scale, airgaps of 1 to 10 μm and overall dimensions less than 1 mm, makes the electrostatic field beneficial compared to the magnetic field. As a consequence, most of these micro devices are electrostatic energy converters. Due to new processes to manufacture microactuators and micromotors as e.g. "X-ray LIGA" Mohr et. al. [1], "Deep UV Lithography" Engelman et. al. [2], "plasma etching" etc. the number of possible structures has grown as well as the precision with which they can be manufactured. Therefore, there is an increasing need for better analysis tools. The demand is for them to be faster and more accurate, but also more flexible and easy to use.

This paper discusses two new techniques for the analysis and the optimisation of electrostatic micromotors of the type variable capacitance motors. The first one is a 3D mesh generation technique for the finite element method (FEM) specially developed for electrostatic micromotors. The second is the generation and use of an equivalent circuit model to enhance and speed up the analysis based on FEM. The paper shows how these techniques have been automated and combined to accomplish optimisation of the average torque of variable capacitance micro motors.

3D Motor Meshes

Building a 3D mesh interactively is a time consuming process. Performing optimisation using interactive 3D FEM is therefore very tedious since numeric optimisation requires a large number of model evaluations. For motor structures, the required labour is even vaster since for every model the analysis must be carried out for a number of rotor positions, in order to obtain macroscopic parameters as functions of the rotor position. For most 3D finite element packages a new rotor position requires a new mesh to be generated. An

automated mesh generation is essential. In this paper an extrusion-based 3D mesh generator is used. It is automated in such a way that a large number of different motor designs can be generated.

Periodic Geometry

All electric rotating motors inherently possess periodicity. Each motor has a stator and a rotor where the geometric period, in degrees, is defined by the pole pitch τ_p. Each periodic design also has an extension within the pole pitch. This extension is referred to as the polar arc τ. For the electrostatic micromotor this is the same as the width of a stator electrode (τ_1) or a rotor tooth (τ_2) (fig. 1). Knowing the pole pitch τ_p and the polar arc τ, the locations of the

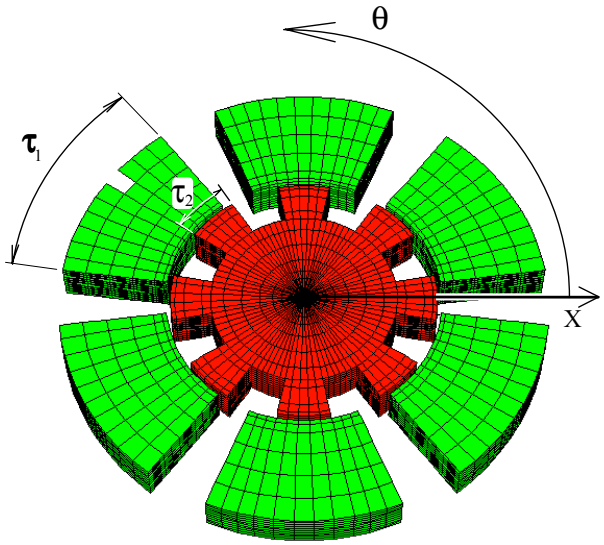

Figure 1: 3D finite element mesh of a 6/8 pole electrostatic radial flux micromotor.

constraining surfaces of the stator electrodes and the rotor teeth are readily calculated. Scanning the motor in the positive θ direction the location of the front-sides and the back-sides of the stator electrodes and the rotor teeth are defined by

$$\left.\begin{aligned}\Theta^n_{front} &= \left(\frac{\tau_p - \tau}{2}\right) + n\cdot\tau_p + \alpha \\ \Theta^n_{back} &= \left(\frac{\tau_p + \tau}{2}\right) + n\cdot\tau_p + \alpha\end{aligned}\right\} \quad n = 0,1,2,\ldots\frac{360° - \tau_p}{\tau_p} \qquad (1)$$

The reference point for θ is chosen in the middle between two stator electrodes. The offset angle α accounts for the rotor position, and is for the stator always zero.

Mesh-extrusion by rotation

The 3D meshes are built using an extrusion technique. With this technique 2D meshes, placed at different locations in space, are generated and connected

resulting in the 3D mesh. A reference 2D mesh is referred to as the baseplane, (fig. 2). Each plane is applied with extrusion data describing its position in space. The extrusion technique, discussed here, uses only rotation around the y-axis, thus θ, to define the extrusion data. One vertical side of each plane coincides with the motor axis being parallel with the global y-axis, (fig. 3).

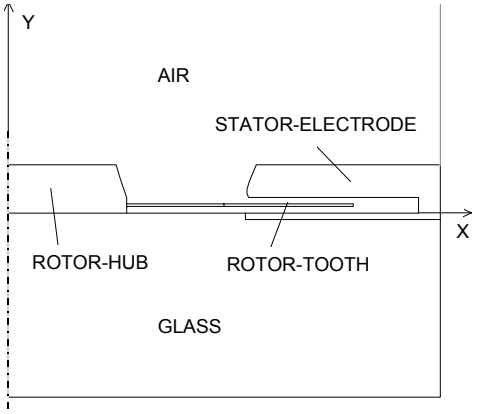

Figure 2: Base-plane used for the generation of the model in figure 3.

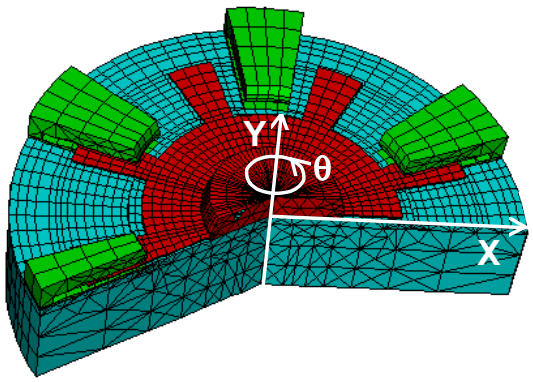

Figure 3: Part of a motor mesh built by altering the material properties, of the planes depending on the angle θ.

For each of the periodic geometric properties in both stator and rotor, 4 different types of actions, sequence of relabeling and/or constraining, are defined. Relabeling indicates material properties and constraining defines equipotential surfaces. Types 1 and 2 define a front and a backside of a stator electrode or a rotor tooth. Types 3 and 4 define a plane inside or outside of ditto. Once the planes are generated the remaining task is to find at what angle which kind of plane must be located. This is performed with repetitive use of (1) and a sorting algorithm.

The angle between two consecutive planes has to be chosen depending on the size of the elements in the base-plane and the required aspect ratio of the 3D elements, the tetrahedrons. The aspect ratio is defined as the ratio of the shortest and the longest side of a tetrahedron. This value must stay within certain limits in order to accomplish a sufficient accuracy of the solving process. This implies that the same kind of planes sometimes has to be repeated with the required angle between them in order to improve the aspect ratio of the tetrahedrons. This is automatically controlled.

Performance of the model generator

The major advantage of automating the extrusion-based mesh generator, rather than using the solid modelling technique, is its speed. To generate a motor model with approximately 100 000 tetrahedrons takes, from the instant that the parameters are entered to the model is ready, less than 10 minutes on a HP715. Once the different kinds of planes are generated, it takes always less than 5

minutes. This should be compared with typically more than 45 min using solid modelling.

The second reason is reliability. The extrusion technique does not make use of any iterative process that for some designs might not converge. If the input data are valid the extrusion technique guaranties a valid mesh. This is very important for an optimisation. Intermediate results not valid due to unsuccessful mesh generation or a total termination of the optimisation process has to be avoided by all means.

Optimisation

One of the most attractive possibilities offered by the automatic mesh generation described, is optimisation. The micromotors from fig. 1 and 3 are modelled by 4 design variables. The free parameters are the number of poles in stator and rotor, and the polar arcs of the stator electrodes and the rotor teeth. However, an optimisation is performed varying only the last two of these design variables. Having a baseplane (fig. 2), the mesh generation technique is automated to generate a 3D motor mesh with the four design variables and the rotor position as the only input.

The optimisation is performed with respect to the average torque which is maximised by varying the two design variables. The average torque is used since the torque is a function of the rotor position and the rotor position for the maximum torque is not constant as the design variables vary. The average torque is calculated using the virtual work technique i.e. exciting one or more of the stator electrodes to a certain voltage, calculating the stored energy for a series of rotor positions and differentiating the gained energy function in order to find the torque function. However, many different excitations, combinations of excited stator electrodes, must be compared. Only if the best excitation for each rotor position is used, the optimisation is meaningful. For each new excitation the finite element program must find a new solution, and thus would an optimisation using only the finite element technique be very time expensive. To overcome this problem an equivalent circuit technique is developed.

Equivalent Circuit Model

The information gained from two different excitations over the rotor positions is sufficient to create an equivalent circuit describing the motor geometry. The equivalent circuit used for a 6/8 pole motor is shown in fig. 4 and consists of 12 capacitors, two times the number of stator electrodes (poles). Their capacitance varies with the rotor position α. There are only two principally different capacitors, or rather capacitance functions. The first type is the function representing the capacitance between each stator electrode and the rotor, $C_k^{SR}(\alpha)$. The second type is the function representing the capacitance between each pair of consecutive stator electrodes $C_k^{SS}(\alpha)$. In $C_k^{SR}(\alpha)$, k represents the

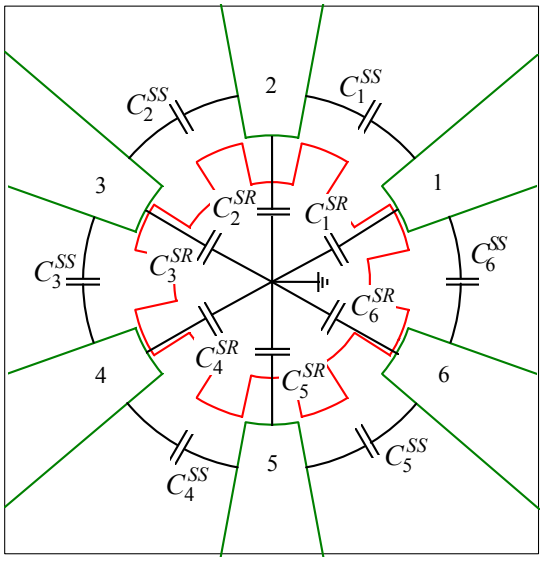

Figure 4. Equivalent circuit for an electrostatic motor with 6 stator poles.

electrode number. In $C_k^{SS}(\alpha)$, k is the number of the first electrode in the pair. Finding the energy stored in a capacitor from (2), and calculating the stored energy in the motor, for two different excitations and for n rotor positions, the system of equations (3) can be solved.

$$W_e = \tfrac{1}{2} C V^2 \tag{2}$$

$$\left.\begin{aligned} W_e(\alpha_1) &= \tfrac{1}{2}\sum_{k=1}^{n_{p1}}\left[C_k^{SR}(\alpha_1)V_k^2 + C_k^{SS}(\alpha_1)\cdot\left(V_{k+1}-V_k\right)^2\right] \\ &\vdots \\ W_e(\alpha_n) &= \tfrac{1}{2}\sum_{k=1}^{n_{p1}}\left[C_k^{SR}(\alpha_n)V_k^2 + C_k^{SS}(\alpha_n)\cdot\left(V_{k+1}-V_k\right)^2\right] \end{aligned}\right\} \tag{3}$$

where: $V_{k+1} = V_1$

n_{p1} = number of stator electrodes

n = number of rotor positions

Once $C_k^{SR}(\alpha)$ and $C_k^{SS}(\alpha)$ are found and made continuous, using discrete FOURIER transform, the torque is calculated by an analytic differentiation.

$$T_V(\alpha) = \frac{\partial W_e(\alpha)}{\partial \alpha} \tag{4}$$

The Best Excitation Sequence

Having the equivalent circuit, any kind of excitation wave form can easily be applied. A block shaped wave form, simulating switching, is applied throughout the optimisation. To avoid or at least minimise radial forces on the rotor shaft, the motors have to be excited symmetrically. Figure 5 shows the possible symmetric excitations of a motor with 6 stator electrodes, where the dark electrodes are excited to V_k Volt and the white electrodes, and the rotor, are set to a reference potential.

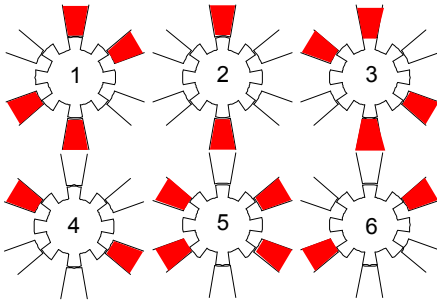

Figure. 5: Possible symmetric excitations of a motor with six electrodes.

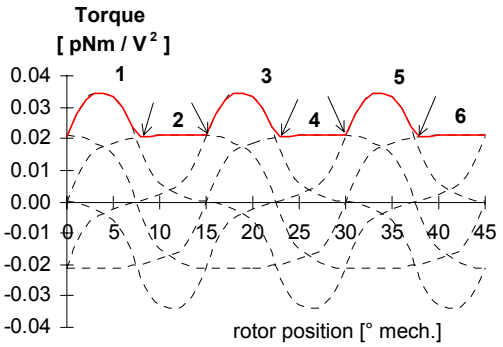

Figure. 6: Static torque over one electric period for 6 different excitations of a 6/8 pole motor.

By applying these excitations to the equivalent circuit, the torque as a function of the rotor position can be calculated. Fig. 6 shows the torque produced over one electric period for the six different excitations from fig. 5. By switching from one excitation to another, at the crossovers marked by the arrows, the optimum excitation sequence is achieved. The average torque T_{av} is then calculated by integrating the curve always following the highest torque. The torque ripple T_{rpl} is given by

$$T_{rpl} = \frac{T_{max} - T_{min}}{T_{av}} \tag{5}$$

Results

Four different types of micromotors have been optimised with respect to maximum average torque. Two radial flux micromotors and two axial flux micromotors. For both types of motors two different pole configurations are considered, the 6/8 pole and the 6/4 pole configuration. For each of these designs the optimisation is performed with respect to the average electric torque and the design variables, the polar arc of both stator and rotor. Due to constraints resulting from the manufacturing conditions the other design variable are set to fixed values. For the radial flux motor (fig. 1) the air gap is

fixed to 10 µm, the rotor height to 100 µm and the outer diameter of the rotor to 600 µm. For the axial flux motor (fig. 3) the air gap is fixed to 3 µm, the rotor thickness to 4 µm and the outer diameter of the rotor to 320 µm. Tables 1 shows the results of the optimisations. Also the motors having the lowest torque ripple from the sample space are listed. An asterisk indicates that the sample lays on the edge of the sample space

Table 1: The normalised average torque of the strongest motors from the optimisation and corresponding geometric parameters.

		T_{av} pNm/V^2	T_{rpl} %	τ_1 ° mech.	τ_2 ° mech.
6/8 pole	max. T_{av}	0.028	63	18.0	21.5
	min. T_{rpl}	0.025	28	18.0	13.5 *
6/4 pole	max. T_{av}	0.035	83	42.0	40.5
	min. Trpl	0.029	26	30.0 *	40.0
6/8 pole	max. T_{av}	0.051	90	18	21.5
	min. Trpl	0.041	40	21.5	13.5
6/4 pole	max. T_{av}	0.060	125	44.5	38
	min. Trpl	0.046	35	54 *	48.5

Table 1 shows that for the radial flux motors, the 6/4 pole configuration is superior to the 6/8 pole. The maximum average torque from the strongest 6/4 pole motor is for the radial flux design 25% higher compared to the strongest 6/8 pole motor. For the axial flux design the difference is 18% in favour of the 6/4 pole motor. Also if only a low torque ripple is concerned the 6/4 pole

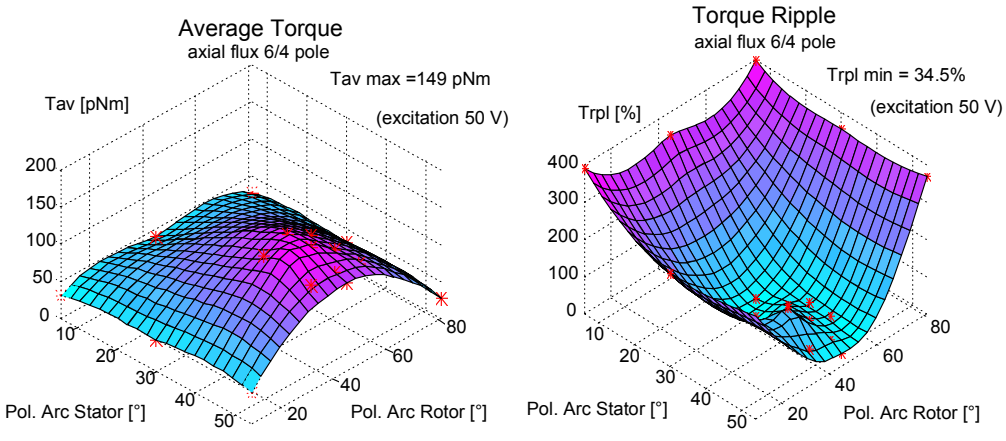

Figure. 7: (A) Average Torque and (B) torque ripple as a function of the polar arc in the stator and the rotor, for 6/4 pole axial flux micromotors.

configuration is the better choice. Figure 7 gives a more clear picture on how the average torque and the torque ripple are depending on the design variables. In these pictures a surface fit has been applied to the evaluated points obtained from the optimisation process of the axial flux 6/4 pole motor. Figure 7A shows that the average torque has one global maximum for the two design variables. Thus, there is one unique combination of the polar arc in the stator and the rotor that results in a higher average torque then any other combination. For the torque ripple the situation is different. Figure 7B shows that the torque ripple does not have a unique global minimum, instead it shows a valley of low torque ripples. Any combinations of the two design variables ending up at the bottom of the valley will give almost the same value of the torque ripple.

Conclusions

This paper describes a technique to automate the generation of 3D meshes for electrostatic micromotors, and explains how this technique combined with an equivalent circuit technique provides the necessary tool to perform an optimisation of motors with respect to the average torque and/or torque ripple. Both the described model generation and equivalent circuit technique are well suited for further development. An optimisation is performed for two different pole configurations of an radial flux and an axial flux design. The results show that the 6/4 pole configuration is able to produce a higher average torque then the 6/8 pole configuration.

Acknowledgements

The authors extend their gratitude to the Belgian Ministry of Scientific Research for granting the IUAP No. 51 on Magnetic Fields. Further we acknowledge the council of the Belgian National Science Foundation. The work is also a part of the Brite/Euram project no. BE 3360.

References

1. J. Mohr, C. Burbaum, P. Bley, W. Menz and U. Wallrabe, 1990, MST '90 pp. 529-537.
2. G. Engelman, O. Ehrmann, R. Leutenbauer, H. Schmitz and H. Reichl, 1993 SPIE 2045, pp. 306-313.
3. W. Trimmer, R. Jebens, "Harmonic Electrostatic Motors", Sensors and Actuators, 20, 1989, pp. 17-224.
4. T.B. Johansson, M. Van Dessel, R. Belmans, W. Geysen, IEEE Trans. on Industry Applications Volume 30 Number 4, pp. 912 - 919.
5. D. A. Lowther P. P. Silvester 1985, "Computer Aided Design in Magnetics" Springer-Verlag, Berlin, New York, Heidelberg, Tokyo.